Appl. Phys. A 66, S875–S878 (1998)

Applied Physics A
Materials
Science & Processing

Theoretical study of the resistance of short $(Xe)_n$ wires within an STM junction: the $(Xe)_2$ case

L. Pizzagalli[1], C. Joachim[2], X. Bouju[3], Ch. Girard[3]

[1] Institut de Physique et de Chimie des Matériaux de Strasbourg, UMR CNRS 46, 23, rue du Loess, F-67037 STRASBOURG, France
(E-mail: pizza@gemme.u-strasbg.fr)
[2] Centre d'Élaboration de Matériaux et d'Études Structurales, UPR CNRS 8011, 29, rue Jeanne-Marvig, B.P. 4347,
F-31055 TOULOUSE CEDEX 4, France
(E-mail: joachim@cemes.cemes.fr)
[3] Laboratoire de Physique Moléculaire, URA CNRS 772, Université de Franche-Comté, F-25030 BESANÇON CEDEX, France
(E-mail : bouju@lpmxb.univ-fcomte.fr)

Received: 25 July 1997/Accepted: 1 October 1997

Abstract. We have theoretically investigated the resistance of two Xe atoms in series in a STM junction, in relation with a previous experimental study [A. Yazdani, D.M. Eigler, and N.D. Lang, Science **272**, 1921 (1996)]. The resistance versus the separation between the STM tip and the surface has been calculated, the relaxation of the Xe atoms being calculated using molecular dynamics. Two major deviations from the well-known exponential decrease of the junction resistance have been found. The first is due to an electronic interference effect. With a tight binding model, we showed that this effect comes from the destructive interference between two different tunneling paths. The second deviation is due to the sideways motion of one Xe atom under the tip compression.

Several experiments made by different groups have recently showed that the tip of the scanning tunneling microscope (STM) can be viewed not only as an observation probe, but also as a nanoscopic tool to manipulate single atoms on a surface [1]. These experiments have opened the way to designing and fabricating diverse nanostructures [2]. Furthermore, the prospect of fabricating nanoscopic electronic devices [3] has increased interest in the characterization of transport properties in these nanostructures [4]. Although transport is well understood at a macroscopic scale, a lot of questions remain unanswered when only a few atoms are involved.

In a recent experiment [5], Yazdani et al. have investigated the electrical resistance of either a single Xe atom or two Xe atoms in series. In the latter case, one Xe is on a Ni(110) surface and the other is adsorbed at the end of the STM tip apex. The Xe atoms are then brought together by decreasing the distance z_{tip} between the STM tip apex and the surface, the resistance versus z_{tip} ($R - z_{\mathrm{tip}}$ characteristic) being recorded.

Yazdani et al. considered that the electrical contact occurred when the resistance begin to saturate at small z_{tip}. The measured resistances are $10^5\ \Omega$ for the single Xe atom and $10^7\ \Omega$ for the two-atom system. However, it must be emphasized that they had no access experimentally to the $(Xe)_2$ wire conformation during the tip approach and therefore they can only have supposed that the two Xe atoms kept their alignment in the STM junction, even for small z_{tip}. Therefore, further calculations are needed before this experiment can be fully understood in relation to the behavior of the Xe atoms at the STM junction. In a recent paper [6], we briefly describe the results of our calculations for one or two Xe atoms, and for the linear $(Xe)_n$ chain. Here, we focus on the two-Xe case. First we show that an electronic interference effect occurs for a medium z_{tip} range. This behavior can be qualitatively explained with a simple tight-binding model. Secondly, the study of the influence of the Xe atoms' relaxation on the $R - z_{\mathrm{tip}}$ characteristic for small z_{tip} is presented. We conclude with an estimation of the resistance of the STM junction equipped with Xe_2, taking into account these two effects.

1 Method

The elastic scattering quantum chemistry (ESQC) method [7] has been used for the determination of the tunneling current through the tip-Xe atoms–surface junction. This method allows us to calculate the transmission coefficient through a defect enclosed in a periodic chain. In our case, the defect is composed of the tip and the Xe atoms, and the model system for the tip body and the surface is a cell semi-infinite in the propagation direction and periodically repeated in the lateral directions. We then used the Landauer formula to obtain the resistance of the system [8]. We must emphasize that the calculated resistance cannot be considered as the intrinsic resistance of the $(Xe)_2$ wire, but almost as the electronic transparence of the electrode–$(Xe)_2$–electrode in the elastic regime [9]. In the ESQC method, the electronic structure is described by an extended Hückel model. Although the absence of self-consistency works against this model, it is particularly suited for this kind of calculation because of the large number of atoms required to describe the junction properly [4].

The periodic cell includes two (110) planes of 5×5 atoms. The tip is a cluster of 10 atoms oriented in the [111] direction, single-atom ended, adsorbed on the (110) surface of the tip body. Yazdani et al. [5] keep an atomic resolution sub-

sequent to the transfer of the Xe from the end of the tip to the surface, indicating that their tip apex is also composed of one single atom at the end. In our calculations, we chose a Cu tip and a Cu(110) surface, instead of the W tip and the Ni(110) surface of their experiment. On one hand, the parametrization of the interactions is better known for the Cu−Xe system than for the Ni−Xe system. On the other hand, the results presented in this paper do not have to be considered as tip or substrate dependent but rather as characteristic of the phenomena which occur during this kind of measure. The electronic structure of the Cu atoms is described by 4*s* orbitals, whereas we have used 6*s* empty and 5*p* filled orbitals for the Xe atoms. These 5*p* orbitals have a non-negligible influence on the tunneling current when the Xe atoms are strongly constrained between the tip and the surface for small z_{tip}.

The positions of the Xe atoms have been calculated by molecular dynamics. We resolve the classical equations of motion using the Verlet algorithm. The interaction energy between the Xe and the surface includes pairwise dipolar and quadrupolar extended Born–Mayer contributions, whereas we used a potential found in the literature for the interaction between the Xe atoms [10]. The last contribution comes from the interaction between the Xe atoms and the tip. A generalized propagator technique have been used to calculate *N*-body dipolar terms, which may become significant according to the tip geometry [11]. For each z_{tip}, we let the two Xe atoms relax until we reach an equilibrium state. The time-averaged positions are then used for the ESQC calculations.

2 Results

Figure 1 shows the $R - z_{tip}$ characteristic as well as the total energy for the $(Xe)_2$ dimer. We also report the experimental data from [5]. The agreement between experimental and calculated curves is clearly excellent, both quantitatively and qualitatively. The theoretical curve can be decomposed into four regions.

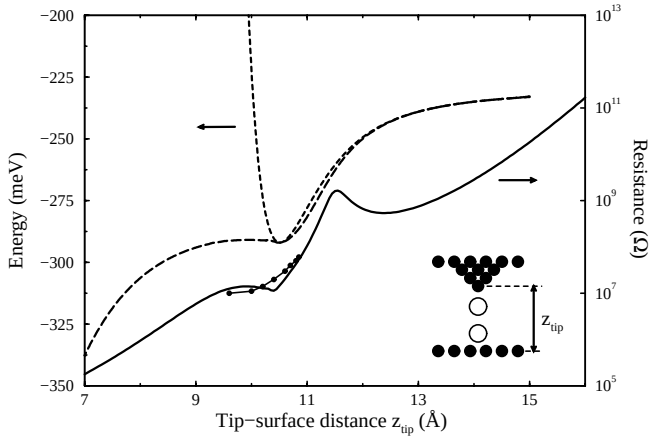

Fig. 1. Variation of the resistance (——) and the total energy (– – –) of the $(Xe)_2$ dimer as a function of z_{tip}. The full and long dashed lines correspond to the free Xe case; the short dashed line shows the total energy when the two Xe are frozen in their stable positions on the surface (2.78 Å) and under the tip (3.43 Å) for large z_{tip}. The black dots correspond to the experimental data from [1]

1. For large z_{tip}, that is for $z_{tip} > 13$ Å, the curve shows the exponential behavior characteristic of a tunnel transport through the $(Xe)_2$ chain. Note that in this case, the two energy curves merge together. This means that the Xe atoms are stable in their starting positions, one Xe being adsorbed at the end of the tip apex and the other on the surface (see insert in Fig. 1).
2. For 10.5 Å $< z_{tip} < 13$ Å, there is a bump in the $R - z_{tip}$ characteristic, although comparison of the two energy curves reveals only small differences. We are always in the attractive regime and the slight shifts of the Xe positions cannot explain this large deviation from standard exponential behavior. The origin of this effect is discussed below.
3. For 9.5 Å $< z_{tip} < 10.5$ Å, the calculated curve shows a saturation similar to the experimental one. The energy for the frozen $(Xe)_2$ dimer increases, whereas for the free dimer it varies approximately like the resistance. The system is now in the repulsive regime. This z_{tip} range will be studied below in the section on mechanical deformations.
4. If $z_{tip} < 9.5$ Å, an exponential decrease is recovered.

3 The interference effect

We have mentioned previously that a bump in the $R - z_{tip}$ characteristic occurs for a z_{tip} range where there are still no mechanical deformations. This bump must therefore be the consequence of an electronic effect. If we remove the 5*p* orbitals of the Xe atoms, the bump is not cancelled but occurs for somewhat different z_{tip}, indicating that only the 6*s* orbitals are involved in this effect. Another test was to remove the 10-atom tip and investigate the resistance variations when two Xe atoms, each located at a constant distance from the Cu(110) slab, were brought together. We still noticed a bump.

To determine what causes such a bump, we have considered a simple tight-binding model (Fig. 2a). The slabs are represented by two semi-infinite chains and the 6*s* atomic orbitals of the Xe atoms by two levels of energy ε. All the couplings between the Xe atoms and the slabs have to be considered to describe the system correctly. These couplings depend on the overlap between electronic wave functions. We then transform the model into an effective one

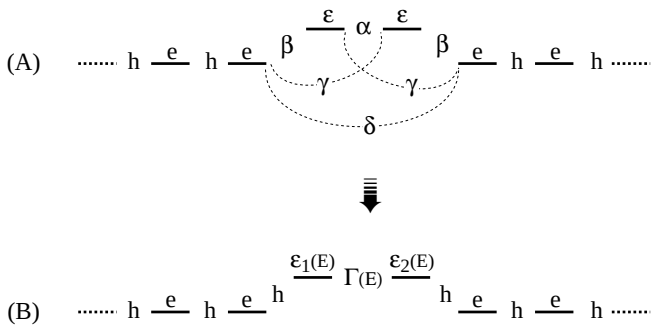

Fig. 2. a Tight binding representation of two Xe atoms in a tunnel junction composed of two slabs. The semi-infinite chains on each side represent the two slabs. ε is the energy level of the 6*s* orbital of the Xe atoms. α, β, γ and δ are respectively the couplings between the Xe atoms, between the slab and the closest Xe atom, between the slab and the more distant Xe atom, and between the two slabs. **b** Effective tight binding model

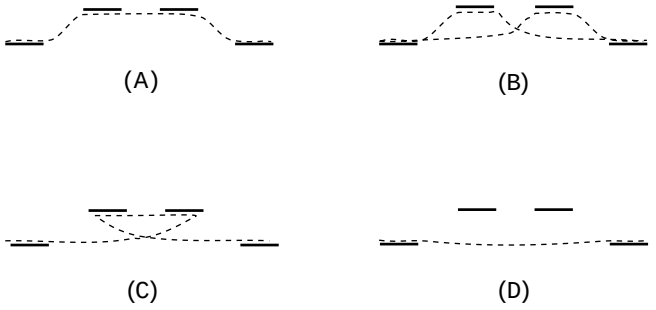

Fig. 3a–d. Schematic picture of the tunneling paths (– – –) through the tight binding model of Fig. 2a. Each path corresponds to one contribution in the expression of the effective coupling $\Gamma(E)$ (Fig. 2b)

which is strictly equivalent (Fig. 2b) [12]. The main advantage of this transformation is that the contributions due to the different couplings are now contained in a single effective energy-dependent coupling $\Gamma(E)$. If the distance between the two slabs is now reduced, the couplings α, γ and δ will be stronger, and therefore the levels $\varepsilon_1(E)$, $\varepsilon_2(E)$ and $\Gamma(E)$ will be modified. The strongest contribution to the variation of the transmission coefficient comes from the variation of the effective coupling $\Gamma(E)$:

$$\Gamma(E) = \frac{\alpha\beta^2}{(E-\varepsilon)^2-\alpha^2} + 2\left[\frac{\gamma\beta(E-\varepsilon)}{(E-\varepsilon)^2-\alpha^2}\right] + \frac{\alpha\gamma^2}{(E-\varepsilon)^2-\alpha^2} + \delta\,. \quad (1)$$

Each term in (1) corresponds to a different transmission channel. For example, $\alpha\beta^2$ in the first term means that the electrons tunnel from the left chain to the left level $\varepsilon(\beta)$, then to the right level $\varepsilon(\alpha)$ and finally to the right chain (β). The different tunneling paths are indicated schematically in Fig. 3. A is the path corresponding to the first term, B to the second term, and so on.

As previously mentioned, the stronger the overlap, the stronger the coupling. For the distances investigated , γ and δ are the weakest couplings, so we neglect the third and the last terms in the expression of $\Gamma(E)$. The electronic transmission now relies only on the tunneling paths A and B (Fig. 3). But the phase shift introduced on the wave function through each of these channels is different. Therefore, the superposition of the two channel contributions at the end of the tunneling path will be destructive for energy lower than ε. This will introduce a decrease of the transmission and then an increase of the elastic resistance.

In Fig. 4, we have plotted the $R-z_{\rm tip}$ curve obtained while the overlap between the two Xe atoms is removed just before calculating the transmission properties. This is equivalent to cancel the α coupling between the two electronic levels ε. The first term in the $\Gamma(E)$ expression vanishes and the bump disappears, confirming the destructive interference effect.

4 Mechanical deformations

If $z_{\rm tip}$ is lower than 10.5 Å, the constraint due to the tip is strong enough to shift the Xe atoms away from their initial positions. It is obvious that the saturation in the $R-z_{\rm tip}$ curve must be correlated with the Xe displacements. However, in order to be sure that no other effects have to be put forward, we plotted in Fig. 4 the $R-z_{\rm tip}$ characteristic for the system with the Xe atoms frozen in their initial positions. In this case, the resistance is clearly no more saturated. The mechanical contact is defined for $z_{\rm tip}$ equal to 10.5 Å, leading to an experimental resistance of about $2\times10^7\,\Omega$. In this $z_{\rm tip}$ range, the Xe $5p$ orbitals must be included in the calculation otherwise the resistance curve is deformed but does not show the same saturation behavior as in the experimental curve. Although the spatial extension of these orbitals is weak in comparison with 6s orbitals, they make a non-negligible contribution to the tunneling current for the short interatomic distances in the repulsive regime.

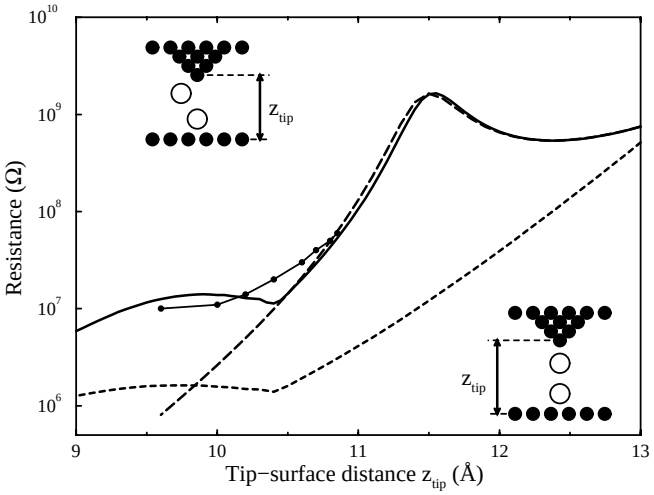

Fig. 4. Variation of the resistance of the $(Xe)_2$ dimer as a function of $z_{\rm tip}$ for a narrower $z_{\rm tip}$ range than in Fig. 1. The full line shows the resistance for two free Xe atoms. The short dashed line corresponds to the case where the overlap between the two Xe atoms is cancelled. The long dashed line shows the resistance calculated for two frozen Xe atoms

Figure 5 represents different configurations during the tip approach. In configuration 1, the Xe atoms are in series between the tip and the surface. Beyond the electrical contact, the Xe at the end of the tip apex begins to move sideways (configuration 2). Then the decrease of the transmitted current through channel A (Fig. 3) because of this shift is solely compensated by the strengthening of the transmission through the channel B due to the tip descent. Therefore the resistance curve saturates. For $z_{\rm tip} < 9.5$ Å, we again found an exponential decrease in the resistance. In this case, the electrons are tunneling from the tip to the surface through one unique Xe atom (configurations 3 and 4), the influence of the other Xe becoming very weak.

Until $z_{\rm tip} = 6.15$ Å, the deformation of the dimer is elastic; i.e. if we raise the tip, the Xe atoms come back to their initial positions. Under this limit, the tip Xe atoms jump to the surface (plastic deformation).

5 Conclusion

We have calculated the transport properties for a $(Xe)_2$ dimer confined in the gap of a STM junction. Our results are in excellent agreement with previous experiment and simulation by Yazdani et al. [5]. In comparison with their calculations,

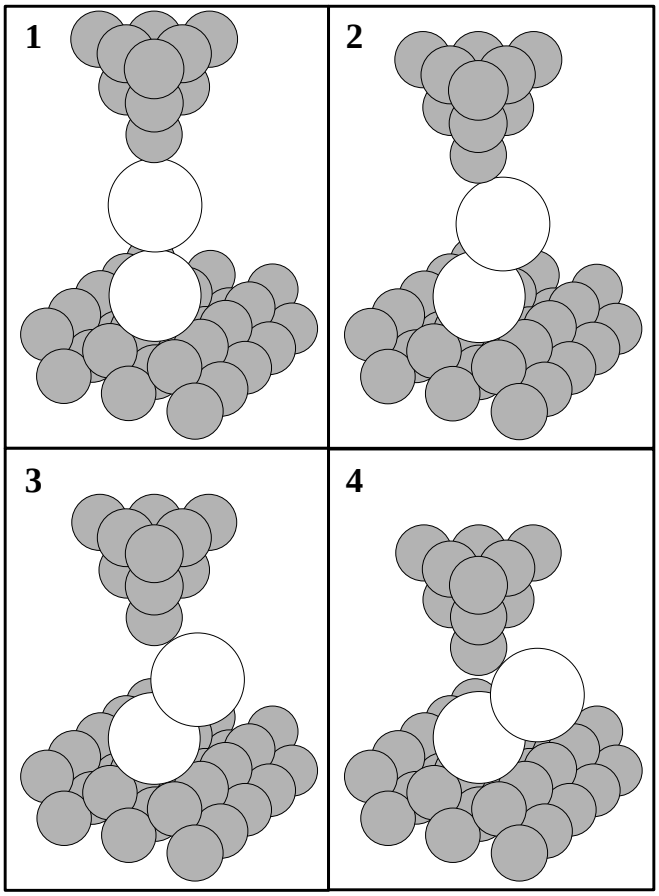

Fig. 5. Snapshots of the atomic positions of the Xe atoms (white circles), the Cu(110) surface, and the tip (grey circles). Only one part of the surface cell is shown; the tip body, where the tip apex is chemisorbed to compute the current, has been removed for clarity. Picture 1 represents the configuration for z_{tip}=11 Å, 2 for $z_{tip} = 10$ Å, 3 for $z_{tip} = 9$ Å and 4 for $z_{tip} = 7.5$ Å

we have included the relaxation of the Xe atoms in the junction during the tip approach. We showed that these dynamical motions must be taken into account for a full understanding of the experimental curve. Moreoveer we have obtained a strong deviation from the exponential decrease of the resistance junction for a z_{tip} range not investigated in the experimental study. We showed using a simple tight binding that this variation is due to an electronic interference effect between two different tunneling channels.

A measure of the resistance of the two Xe in series requires that z_{tip} is greater than 10.5 Å, which is the upper bound before deformation. For $z_{tip} > 10.5$ Å, we have to deal with the electronic interference effect and therefore the resistance can only be estimated. We estimate that the resistance ranges from 10 MΩ to 30 MΩ.

References

1. D.M. Eigler, E.K. Schweizer: Nature **344**, 524 (1990); L.J. Whitman, J.A. Stroscio, R.A. Dragoset, R.J. Celotta: Science **251**, 1206 (1991); I.-W. Lyo, P. Avouris: Science **253**, 173 (1991); D.M. Eigler, C.P. Lutz, W.E. Rudge: Nature **352**, 600 (1991); J.A. Stroscio, D.M. Eigler: Science **254**, 1319 (1991); D. Eigler: *Atomic and Nanometer-Scale Modification of Materials: Fundamentals and Applications*, Vol. 239 of *NATO ASI Series E: Applied Sciences* (Plenum Press, Dordrecht 1993) p. 1; T.A. Jung, R.R. Schlitter, J.K. Gimzewski, H. Tang, C. Joachim: Science **271**, 181 (1996); G. Meyer, S. Zöphel, K.-H. Rieder: Phys. Rev. Lett. **77**, 2113 (1996)
2. P. Zeppenfeld, C.P. Lutz, D.M. Eigler: Ultramicroscopy **42**–**44**, 128 (1992); M.F. Crommie, C.P. Lutz, D.M. Eigler: Science **262**, 218 (1993); M.T. Cuberes, M.R. Schlittler, J.K. Gimzewski: Appl. Phys. Lett. **69**, 3016 (1996)
3. C. Joachim, J.K. Gimzewski: Chem. Phys. Lett. **265**, 353 (1997)
4. C. Joachim, J.K. Gimzewski, R.R. Schlitter, C. Chavy: Phys. Rev. Lett. **74**, 2102 (1995)
5. A. Yazdani, D.M. Eigler, N.D. Lang: Science **272**, 1921 (1996)
6. L. Pizzagalli, C. Joachim, X. Bouju, C. Girard: Europhys. Lett. **38**, 97 (1997)
7. C. Joachim, P. Sautet, P. Lagier: Europhys. Lett. **20**, 697 (1992)
8. R. Landauer: Z. Phys. B **68**, 217 (1987); R. Landauer: *Nanostructure Physics and Fabrication, Proceedings of the International Symposium, College Station, Texas* (Academic Press, San Diego (1989) p. 17
9. C. Joachim, J.F. Vinuesa: Europhys. Lett. **33**, 635 (1996)
10. A.D. Koutselos, E.A. Mason, L.A. Viehland: J. Chem. Phys. **93**, 7125 (1990)
11. X. Bouju, Ch. Girard, H. Tang, C. Joachim, L. Pizzagalli: Phys. Rev. B **55**, 16498 (1997)
12. C. Joachim: Ph.D. thesis, Université Paul Sabatier, Toulouse (1990)